# Buckling Behavior of a Functionally Graded Sandwich Plate

**Anil Kumar Gupta**
Department of Civil Engineering, National Institute of Technology Patna, India
anilguptakeck@gmail.com (corresponding author)

**Ajay Kumar**
Department of Civil Engineering, National Institute of Technology Delhi, India
sajaydce@gmail.com

*Received: 16 May 2023 | Revised: 27 May 2023 | Accepted: 28 May 2023*

 *DOI: https://doi.org/10.48084/etasr.6059*

**ABSTRACT**

**This research focuses on the buckling behavior of a porous Functionally Graded (FG) sandwich plate using the sinusoidal shear deformation theory and hyperbolic tangent and secant thickness stretching functions with novel displacement fields. The proposed model assumes a different thickness layer system with FGM on the top and bottom and a ceramic core. Hamilton's energy principle is applied to the FGM sandwich plates to understand their buckling behavior. The mesh convergence on Finite Element (FE) model is carried out, and the accuracy of the results is tested using the existing research. The present model results match reasonably well with the previously published literature. The impact of the transverse shear deformation, plate aspect ratio, size-to-thickness ratio, and volume fraction is investigated for different thickness layer systems.**

***Keywords-FG sandwich plate; finite element method; critical buckling load***

## I. INTRODUCTION

Composite structures are highly demanding due to mechanical properties such as endurance, light weight, high strength, and stiffness to mass ratios. They are employed in numerous modern engineering applications, including civil construction, vehicles, marine industry, and aerospace applications. Understanding the mechanical behavior of composite laminates is essential for the intricate design since composite laminates can be customized to serve the intended purpose while having a very complicated composition due to their layered structure. Functionally graded composites are able to carry out contemporary and unique tasks that traditional composite materials are unable to. These sophisticated composite materials, which are manufactured using advanced combinations of metal and ceramic techniques, have microscopically inhomogeneous morphology [1].

Exploring optimal materials that fulfil the strength and stability standards over their lifetime is a tough work for an engineer due to the rising demands given by the numerous structural components. Composites are increasingly preferred in this context due to the amount of flexibility they provide in terms of product design. High stiffness and strength may be achieved with a minimal weight by using a variety of lamination schemes, fibre orientation, material types, and material combinations. Nowadays, numerous types of engineering structures use Functionally Graded (FG) sandwich plates. In order to achieve improved mechanical characteristics in traditional laminated composite materials, homogeneous elastic laminae are joined to one another. However, a sudden shift in material characteristics at the interface between two materials may result in high interlaminar stresses, which may lead to delamination. The use of FGMs, where material characteristics vary continuously, is one method to counteract these negative effects. This can be implemented by varying the volume fraction of the constituent materials progressively, typically along the thickness direction. This reduces interface-related problems of composites, resulting in uniform stress distributions. Generally, FGMs are composed of a composition of ceramic and metal or made up of different materials. The ceramic component in a FGM provides temperature barrier effects and prevents the metal from corrosion and oxidation, while the metallic component toughens and reinforces the FGM [2-4]. Due to widespread use of FG sandwich structures, it has become essential to know their responses. Shear deformation theories like the First-Order Shear Deformation Theory (FSDT) and Higher-Order Shear Deformation Theory (HSDT) need to be implemented to predict the responses of FG sandwich plates, as the shear deformation effect is more noticeable in thick plates or plates composed of novel materials such as FGM. The FSDT offers good results, but they rely on the shear modification factor, which is challenging to figure out because it involves a number of variables. On the other hand, HSDT doesn't need a shear modification factor, but its equations of motion are more difficult compared to FSDT [5]. From the 3-D equations of elasticity, a 2-D theory of bending movements of isotropic, elastic plates can be made. Like Timoshenko's one-dimensional theory of bars, this theory takes into account the effects of rotatory inertia and shear [6]. Authors in [7] proposed a mathematical 3D elasticity solution for a sandwich hybrid with a FG core, loaded by a hard sphere indentor in a crosswise direction. On the basis of first order shear deformation theory and nonlinear von Karman displacement field with variable thickness under uniform temperature rise, the thermal stability of a sandwich FGM circular plate with variable thickness has been analysed in [8]. The buckling behavior of FGM circular plates with variable thickness under radial compression has been investigated in [9]. Under thermal and mechanical loadings, authors in [10] conducted buckling analysis of truncated conical sandwich FGM shells with stiffeners and various material combinations along the thickness supported by Pasternak elastic foundations under thermal and mechanical loadings. The four-node quadrilateral element for plates based on third order zigzag theory was improved in [11] and was validated by static and dynamic behavior. The inverse hyperbolic shear deformation theory based on $C_0$ continuity Finite Element (FE) technique has been proposed for the analysis of sandwich plates and laminated composites in [12]. Unified formulation has been extended to FGM plates, and a variable kinematic model taking into account different material laws along the thickness was proposed in [13]. The $C_0$ isoparametric element and Mori-Tanaka homogenization technique have been used to conduct static and dynamic analyses on FGM skew plates exposed to mechanical pressure in [14]. The impact of skew angle on the axial stress and deflection has been studied employing the same Lagrangian element in combination with higher order shear deformation theory in [15].

The buckling of FGM sandwich plates is analyzed in this study using the equivalent single layer shear deformation theory. In order to take into consideration the shear deformation in the displacement field, a modified hyperbolic function in terms of thickness direction was used. To evaluate the buckling behavior of FGM sandwich plates, an FE model has been created. The $C_0$ FE model was developed based on a new mathematical model to facilitate buckling analysis and was evaluated for convergence. The outcome has been corroborated by previously published research. The buckling behavior has been analyzed using parametric studies to assess the impact of different material layers with various thicknesses by varying size to thickness ratio, power index, and aspect ratio.

## II. FORMULATION

### *A. Geometry of the FGM Sandwich Plate*

The geometrical features of a sandwich plate (with FGM on top and bottom surface and ceramic core) are described in Figure 1 with sides a and b and total thickness h. The mid-plane of the plate is taken as the reference plane (z = 0).

### *B. Homogenization of the FG Plate*

The volume fraction function is defined in (1), with the power index (p) and the distance from the mid-plane (z) of the plate.

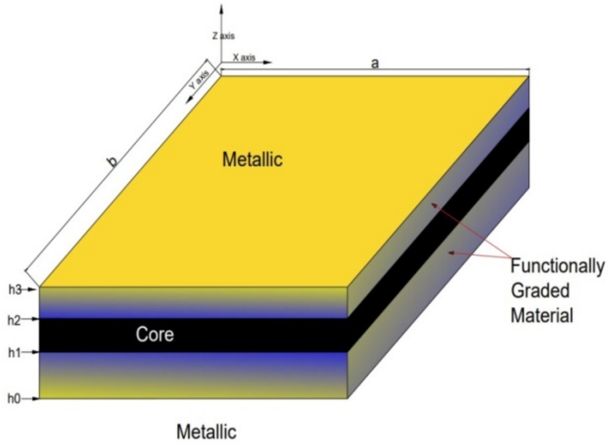


Fig. 1. Geometry of the FGM sandwich plate.

Effective material parameters like Young's modulus $E(z)$ and Poisson ratio $\mu(z)$ can be determined as functions of thickness for different thickness layer systems from mid-plane as follows:

$$V_1(z) = \left\{\frac{z-h_0}{h_1-h_0}\right\}^p \quad (1a)$$

here, z lies between $h_0$ and $h_1$.

$$V_2(z) = 1 \quad (1b)$$

here, z lies between $h_1$ and $h_2$.

$$V_3(z) = \left\{\frac{z-h_3}{h_2-h_3}\right\}^p \quad (1c)$$

here, z lies between $h_2$ and $h_3$.

$$E(z) = E_m + (E_C - E_m) * V_n(z) \quad (2a)$$

$$\mu(z) = \mu_m + (\mu_C - \mu_m) * V_n(z) \quad (2b)$$

where $E_m$, $\mu_m$, and $E_C$, $\mu_C$ represent Young's modulus and Poission's ratio of metal and ceramic, respectively. Power index is denoted by $p \geq 0$, $V_n(z)$ is the volume fraction function of layer n (n = 1, 2, 3) at thickness z.

The suggested HSDT uses the shear deformation function g(z) associated with $\psi_{sx}$ and $\psi_{sy}$ which is represented in (3), whereas the transverse shear strain distribution along plate thickness, thickness stretching function t(z) associated with $\Phi$ is expressed in (4) to include the thickness stretching deformation of plate.

$$g(z) = \frac{h}{\pi}\sin\left\{\frac{\pi z}{h}\right\} \quad (3)$$

$$t(z) = \left\{\frac{3\pi}{2}\right\}\left(1 - \tanh^2\frac{z}{h}\right) - \frac{3\pi}{2}\operatorname{sech}^2\frac{1}{2} \quad (4)$$

In-plane displacements u, v, and transverse displacement w are expressed in (5)-(7) using the shape function g(z) and the thickness stretching function t(z). For the $C_0$ continuity of the FE analysis, out of plane derivatives are complex due to the involvement of the strain with second-order derivatives, but $C_1$ continuity is extremely intricate and difficult to model. Therefore, new nodal unknowns are substituted for the out-of-plane derivatives to verify that displacement field variables are continuous within elements and need the application of penalty approach during FE formulation.

$$u(x,y,z) = u_0(x,y) - z\alpha_{bx}(x,y) - g(z)\psi_{sx}(x,y) \quad (5)$$

$$v(x,y,z) = v_0(x,y) - z\alpha_{by}(x,y) - g(z)\psi_{sy}(x,y) \quad (6)$$

$$w(x,y,z) = w_0(x,y) + t(z)\Phi(x,y) \quad (7)$$

where $\alpha_{bx} - \frac{\partial w}{\partial x} = 0,\ \alpha_{by} - \frac{\partial w}{\partial y} = 0.$

## *C. Kinematics of Structure*

Strain–displacement can be derived by differentiating the displacement field as given below:

$$\epsilon_{xx} = \frac{\partial u_o}{\partial x} - z\frac{\partial \alpha_{bx}}{\partial x} - g(z)\frac{\partial \psi_{sx}}{\partial x}$$

$$\epsilon_{yy} = \frac{\partial v_o}{\partial y} - z\frac{\partial \alpha_{by}}{\partial y} - g(z)\frac{\partial \psi_{sy}}{\partial y}$$

$$\epsilon_{zz} = \frac{\partial t_z}{\partial z}\Phi \quad (8)$$

$$\gamma_{xy} = \left\{\frac{\partial u_o}{\partial y} + \frac{\partial v_o}{\partial x}\right\} - z\left\{\frac{\partial \alpha_{bx}}{\partial y} + \frac{\partial \alpha_{by}}{\partial x}\right\} - g(z)\left\{\frac{\partial \psi_{sx}}{\partial y} + \frac{\partial \psi_{sy}}{\partial x}\right\}$$

$$\gamma_{xz} = \frac{\partial w_0}{\partial x} - \alpha_{bx} - \frac{\partial f_z}{\partial z}\psi_{sx} + t(z)\frac{\partial \Phi}{\partial x}$$

$$\gamma_{yz} = \frac{\partial w_0}{\partial y} - \alpha_{by} - \frac{\partial f_z}{\partial z}\psi_{sy} + t(z)\frac{\partial \Phi}{\partial y}$$

## *D. Constitutive Relations for the FGM Sandwich Plate*

Linear constitutive relationship between stresses and strain is given by constitutive matrix.

$$Q_{11} = Q_{22} = Q_{33} = \frac{E(z)(1-\mu^2)}{1-3\mu^2-2\mu^3}$$

$$Q_{12} = Q_{13} = Q_{23} = \frac{E(z)\mu(1+\mu)}{1-3\mu^2-2\mu^3}$$

$$Q_{44} = Q_{55} = Q_{66} = \frac{E(z)}{2(1+\mu)} \quad (9)$$

$$\begin{Bmatrix} \sigma_{xx} \\ \sigma_{yy} \\ \sigma_{zz} \\ \tau_{xy} \\ \tau_{xz} \\ \tau_{yz} \end{Bmatrix} = \begin{bmatrix} Q_{11} & Q_{12} & Q_{13} & 0 & 0 & 0 \\ Q_{12} & Q_{22} & Q_{23} & 0 & 0 & 0 \\ Q_{13} & Q_{23} & Q_{33} & 0 & 0 & 0 \\ 0 & 0 & 0 & Q_{44} & 0 & 0 \\ 0 & 0 & 0 & 0 & Q_{55} & 0 \\ 0 & 0 & 0 & 0 & 0 & Q_{66} \end{bmatrix} \begin{Bmatrix} \epsilon_{xx} \\ \epsilon_{yy} \\ \epsilon_{zz} \\ \gamma_{xy} \\ \gamma_{xz} \\ \gamma_{yz} \end{Bmatrix} \quad (10)$$

## *E. Governing Equation of Motion*

Hamilton's principle derives the equations of motion. U is the strain energy, K is the Kinetic energy, and W is the work done by external forces.

$$\oint \delta(U - K - W)\,\partial\Omega = 0 \quad (11)$$

The strain energy of FGM sandwich plate is shown in (12):

$$U = \frac{1}{2}\iiint \epsilon^T \sigma\,\partial x\,\partial y\,\partial z =$$

$$\frac{1}{2}\iint \epsilon_0{}^T\{\int Z^T[Q_{ij}]Z\,\partial z\}\epsilon_0\,\partial x\,\partial y \quad (12)$$

Critical buckling load along the x and y axis is represented by Nx and Ny, while Nxy represents the shear buckling. The total work done by external compressive forces acting on the plate edges is:

$$W = \frac{1}{2}\iiint \left\{N_x \frac{\partial w^2}{\partial x} + N_y \frac{\partial w^2}{\partial y} + 2N_{xy}\frac{\partial w}{\partial x}\frac{\partial w}{\partial y}\right\} dxdydz \quad (13)$$

The material rigidity matrix [D] is obtained from the constitutive matrix given in (10) and the thickness matrix given in (14). This matrix facilitates the use of the proposed HSDT as an equivalent single layer theory to downscale the 3-D domain to the 2-D domain for the analysis.

$$[Z] =$$

$$\begin{bmatrix} 1 & 0 & 0 & 0 & 0 & z & 0 & 0 & 0 & 0 & g_z & 0 & 0 & 0 & 0 & 0 & 0 & 0 \\ 0 & 1 & 0 & 0 & 0 & 0 & z & 0 & 0 & 0 & 0 & g_z & 0 & 0 & 0 & 0 & 0 & 0 \\ 0 & 0 & 0 & 0 & 0 & 0 & 0 & 0 & 0 & 0 & 0 & 0 & 0 & 0 & 0 & t'_z & 0 & 0 \\ 0 & 0 & 1 & 0 & 0 & 0 & 0 & z & 0 & 0 & 0 & 0 & g_z & 0 & 0 & 0 & 0 & 0 \\ 0 & 0 & 0 & 1 & 0 & 0 & 0 & 0 & 1 & 0 & 0 & 0 & 0 & g'_z & 0 & 0 & t_z & 0 \\ 0 & 0 & 0 & 0 & 1 & 0 & 0 & 0 & 0 & 1 & 0 & 0 & 0 & 0 & g'_z & 0 & 0 & t_z \end{bmatrix} \quad (14)$$

$$[D] = \int_{z=-h/2}^{z=h/2} [Z]^T [Q_{ij}][Z]\,\partial z \quad (15)$$

The geometric rigidity matrix $[D_G]$ is obtained by $[\widehat{N}]$ and thickness coordinate matrix $[Z_b]$ given in (16):

$$[D_G] = \int_{z=-h/2}^{z=h/2} [Z_b]^T [\widehat{N}][Z_b]\,\partial z \quad (16)$$

where:

$$[\widehat{N}] = \begin{bmatrix} N_x & N_{xy} \\ N_{xy} & N_y \end{bmatrix}$$

$$[Z_b] = \begin{bmatrix} 1 & 0 \\ 0 & 1 \\ t(z) & 0 \\ 0 & t(z) \end{bmatrix}$$

Thee displacement in the FE can be represented as the linear combination of node shapes and corresponding shape functions. The principle of virtual work was applied using the mid plane strain vector. The material stiffness matrix and the geometrical stiffness matrix are obtained. The total potential energy for buckling analysis is:

$$\pi_N = \frac{1}{2}\iint \epsilon_0{}^T[D]\,\epsilon_0\,\partial x\,\partial y - \frac{1}{2}\iint \epsilon_b{}^T[D_G]\,\epsilon_b\,\partial x\,\partial y \quad (17)$$

$$[K_G] = \iint [B_B]^T[D_G][B_B]\,[J]\,\partial\zeta\,\partial\eta \quad (18)$$

# III. RESULTS AND DISCUSSION

In the current work, buckling analysis on FGM sandwich plate was carried out using FE formulation based on a 9-node isoparametric $C_0$ continuous shape function.

## *A. Model Convergence and Validation*

Based on the suggested innovative HSDT, the governing equations for the FE model which is utilized for the buckling analysis of the FGM sandwich plate are obtained from the principle of virtual work. In-house MATLAB algorithm for FE formulation was written using the 9-noded Lagrangian isoparametric shape functions. Using mesh convergence studies, the FE model was evaluated and its performance was assessed. The FE analysis was carried out on a simply supported square FGM sandwich plate. The material properties are shown in Table I. To predict the buckling responses of the FGM sandwich plate, we consider the plate subjected to axial in-plane forces.

TABLE I. MATERIAL PROPERTIES

| Material | Poission's ratio | Mass density ($kg/m^3$) | Modulus of elastiity (GPa) |
|---|---|---|---|
| $Al_2O_3$ | 0.3 | 2702 | 70 |
| Al | 0.3 | 3800 | 380 |

The change in dimensionless critical buckling load with various power law indices, different layers of different thickness types of FGM sandwich and mesh sizes was investigated. The presented numerical solutions are computed using novel theory, and the findings are compared with the existing research. The non-dimensional critical buckling ratio is expressed as:

$$N_{cr} = \frac{Na^2}{E_m h^3}$$

where N is the buckling load due to external load. From Table II, it can be seen that as power index increases, the non-dimensional critical buckling loads for uniaxial and biaxial compression loading for different thickness layer systems decrease. It can be seen that for various layer configurations and for the same boundary condition, non-dimensional critical buckling load decreases with increase in the power index that corresponds to increase in metallic volume fraction. Further, it can be seen that the biaxial buckling loads are smaller than the uniaxial buckling loads. For convergence investigations, several mesh sizes have been used, and the results are reported in Table II in terms of non-dimensional critical buckling load. For validation and accuracy, the model's results were compared to the findings of [5]. For a critical buckling load, it has been observed that a mesh size of 9×9 elements can provide sufficient convergence.

In Table III, the dimensionless critical buckling load for uniaxial and biaxial compressive loading is presented for various power index and aspect ratios for different thickness layer systems, showing that the decrease in the shorter dimension increases the critical buckling load. The $Al/Al_2O_3$ FGM sandwich plate has been analyzed for buckling with all sides simply-supported (SSSS). It has been observed that with a given size-to-thickness (a/h) ratio, a rise in power index results in a gradual decrease in non-dimensional critical buckling load. Further, it is also observed that an increase in (a/b) ratio results in an increase in the critical buckling load for a fixed power index. From Figure 2, it can be seen that the material variation is continuous within the layers of FGM and core, however, there is a drastic change near the layer interface.

TABLE II. NON-DIMENSIONAL CRITICAL BUCKLING LOADS FOR VARIOUS THICKNESS OF LAYER SYSTEMS FOR $Al/Al_2O_3$ FGM SANDWICH PLATE (a/b=1, a/h=10)

| p | Theory | Ref. | Uniaxial buckling load | | | | | Biaxial buckling load | | | | |
|---|---|---|---|---|---|---|---|---|---|---|---|---|
| | | | 1-0-1 | 2-1-2 | 1-1-1 | 2-2-1 | 1-2-1 | 1-0-1 | 2-1-2 | 1-1-1 | 2-2-1 | 1-2-1 |
| 0 | FSDT | [5] | 13.0045 | 13.0045 | 13.0045 | 13.0045 | 13.0045 | 6.5022 | 6.5022 | 6.5022 | 6.5022 | 6.5022 |
| | Present | 5×5 | 13.1092 | 13.1092 | 13.1092 | 13.1092 | 13.1092 | 6.5546 | 6.5546 | 6.5546 | 6.5546 | 6.5546 |
| | Present | 7×7 | 13.0768 | 13.0768 | 13.0768 | 13.0768 | 13.0768 | 6.5384 | 6.5384 | 6.5384 | 6.5384 | 6.5384 |
| | Present | 9×9 | 13.0687 | 13.0687 | 13.0687 | 13.0687 | 13.0687 | 6.5344 | 6.5344 | 6.5344 | 6.5344 | 6.5344 |
| 0.5 | FSDT | [5] | 7.3634 | 7.9403 | 8.4361 | 8.8095 | 9.2162 | 3.6817 | 3.9702 | 4.2181 | 4.4047 | 4.6081 |
| | Present | 5×5 | 7.4329 | 8.0147 | 8.5142 | 8.9265 | 9.2994 | 3.7165 | 4.0073 | 4.2571 | 4.4632 | 4.6497 |
| | Present | 7×7 | 7.4094 | 7.9894 | 8.4879 | 8.8991 | 9.2717 | 3.7047 | 3.9947 | 4.2439 | 4.4495 | 4.6359 |
| | Present | 9×9 | 7.4034 | 7.9830 | 8.4811 | 8.8921 | 9.2647 | 3.7018 | 3.9916 | 4.2406 | 4.4460 | 4.6323 |
| 1 | FSDT | [5] | 5.1648 | 5.8387 | 6.4641 | 6.9485 | 7.5056 | 2.5824 | 2.9193 | 3.2320 | 3.4742 | 3.7528 |
| | Present | 5×5 | 5.2193 | 5.8998 | 6.5306 | 7.1000 | 7.5801 | 2.6097 | 2.9499 | 3.2653 | 3.5500 | 3.7900 |
| | Present | 7×7 | 5.2005 | 5.8785 | 6.5076 | 7.0748 | 7.5485 | 2.6002 | 2.9392 | 3.2538 | 3.5374 | 3.7775 |
| | Present | 9×9 | 5.1956 | 5.8730 | 6.5016 | 7.0683 | 7.5483 | 2.6002 | 2.9365 | 3.2508 | 3.5342 | 3.7742 |

TABLE III. NON-DIMENSIONAL CRITICAL BUCKLING LOAD FOR VARIOUS ASPECT RATIO AND POWER INDEX FOR VARIOUS THICKNESS OF LAYER SYSTEMS FOR $Al/Al_2O_3$ FGM SANDWICH PLATE (a/h = 10)

| p | (a/b) ratio | Uniaxial buckling load | | | | | | Biaxial buckling load | | | | | |
|---|---|---|---|---|---|---|---|---|---|---|---|---|---|
| | | 1-0-1 | 2-1-2 | 2-1-1 | 1-1-1 | 2-2-1 | 1-2-1 | 1-0-1 | 2-1-2 | 2-1-1 | 1-1-1 | 2-2-1 | 1-2-1 |
| 0 | 1/3 | 4.1276 | 4.1276 | 4.1276 | 4.1276 | 4.1276 | 4.1276 | 3.7148 | 3.7148 | 3.7148 | 3.7148 | 3.7148 | 3.7148 |
| | 1/2 | 5.2049 | 5.2049 | 5.2049 | 5.2049 | 5.2049 | 5.2049 | 4.1639 | 4.1639 | 4.1639 | 4.1639 | 4.1639 | 4.1639 |
| | 3/2 | 28.8668 | 28.8668 | 28.8668 | 28.8668 | 28.8668 | 28.8668 | 10.2921 | 10.2921 | 10.2921 | 10.2921 | 10.2921 | 10.2921 |
| | 2 | 45.4834 | 45.4834 | 45.4834 | 45.4834 | 45.4834 | 45.4834 | 15.1822 | 15.1822 | 15.1822 | 15.1821 | 15.1822 | 15.1821 |
| 0.5 | 1/3 | 2.3214 | 2.5035 | 2.6105 | 2.6611 | 2.7934 | 2.9099 | 2.0894 | 2.2533 | 2.3496 | 2.3950 | 2.5144 | 2.6189 |
| | 1/2 | 2.9308 | 3.1607 | 3.2941 | 3.3591 | 3.5250 | 3.6726 | 2.3444 | 2.5285 | 2.6352 | 2.6873 | 2.8201 | 2.9381 |
| | 3/2 | 16.893 | 18.2031 | 18.8385 | 19.2964 | 20.1193 | 20.9776 | 5.8870 | 6.3466 | 6.6030 | 6.7384 | 7.0589 | 7.3506 |
| | 2 | 26.8601 | 28.9383 | 29.9475 | 30.6591 | 31.9572 | 33.2872 | 8.7949 | 9.4791 | 9.8527 | 10.0520 | 10.5227 | 10.9493 |
| 1 | 1/3 | 1.6242 | 1.8360 | 1.9832 | 2.0337 | 2.2171 | 2.3645 | 1.4616 | 1.6525 | 1.7851 | 1.8303 | 1.9952 | 2.1281 |
| | 1/2 | 2.0516 | 2.3190 | 2.5018 | 2.5684 | 2.7971 | 2.9855 | 1.6413 | 1.8552 | 2.0015 | 2.0547 | 2.2377 | 2.3884 |
| | 3/2 | 12.0322 | 13.6020 | 14.4529 | 15.0143 | 16.1370 | 17.3085 | 4.1485 | 4.6895 | 5.0446 | 5.1874 | 5.6333 | 6.0104 |
| | 2 | 19.2013 | 21.7087 | 23.0957 | 23.9486 | 25.7529 | 27.5610 | 6.2321 | 7.0453 | 7.5701 | 7.7853 | 8.4426 | 8.9974 |

## IV. CONCLUSIONS

The buckling behavior of FGM sandwich plates was carried out using FE formulation based on a 9-node isoparametric $C_{00}$ continuous shape function from the novel suggested displacement fields with a hybrid hyperbolic tangent and secant function for accounting for the effect of thickness stretching.

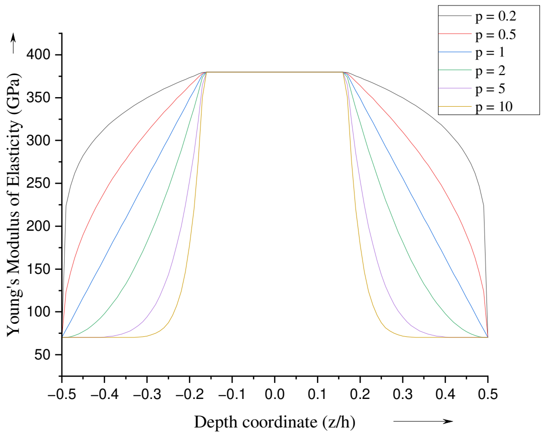


Fig. 2. Variation of Young's modulus with thickness coordinates for various values of power index in the 1-1-1 layer system.

The performance of the FE model is characterized as quite satisfactory after the comparison with the findings of the existing literature. For the parametric study, the model is transformed for different (a/b) ratios and power index. The corresponding critical buckling loads for uniaxial and biaxial compressive loading were calculated. The following key points have been made regarding the critical buckling load in the buckling analysis:

- The developed FE model shows good convergence with an optimal mesh size of 9×9 elements, producing accurate results.
- For the same boundary conditions and plate geometry, the critical buckling load for uniaxial buckling is greater than biaxial buckling.
- The developed FE model delivers results comparable with the existing ones.
- The FG sandwich plate's critical buckling load increases as the ceramic constituent in the plate increases.
- Increase in the (a/b) ratio results in higher values of non-dimensional critical buckling load for a constant power index.

## REFERENCES

[1] I. Kayabasi, G. Sur, H. Gokkaya, and Y. Sun, "Functionally Graded Material Production and Characterization using the Vertical Separator Molding Technique and the Powder Metallurgy Method," *Engineering, Technology & Applied Science Research*, vol. 12, no. 4, pp. 8785–8790, Aug. 2022, https://doi.org/10.48084/etasr.5025.

[2] A. M. Zenkour, "A comprehensive analysis of functionally graded sandwich plates: Part 1—Deflection and stresses," *International Journal of Solids and Structures*, vol. 42, no. 18, pp. 5224–5242, Sep. 2005, https://doi.org/10.1016/j.ijsolstr.2005.02.015.

[3] P. Kumar and A. Kumar, "Free Vibration Analysis of Steel-Concrete Pervious Beams," *Engineering, Technology & Applied Science Research*, vol. 13, no. 3, pp. 10843–10848, Jun. 2023, https://doi.org/10.48084/etasr.5913.

[4] A. K. Gupta and A. Kumar, "Buckling Analysis of Porous Functionally Graded Plates," *Engineering, Technology & Applied Science Research*, vol. 13, no. 3, pp. 10901–10905, Jun. 2023, https://doi.org/10.48084/etasr.5943.

[5] H.-T. Thai, T.-K. Nguyen, T. P. Vo, and J. Lee, "Analysis of functionally graded sandwich plates using a new first-order shear deformation theory," *European Journal of Mechanics - A/Solids*, vol. 45, pp. 211–225, May 2014, https://doi.org/10.1016/j.euromechsol.2013.12.008.

[6] R. D. Mindlin, "Influence of Rotatory Inertia and Shear on Flexural Motions of Isotropic, Elastic Plates," *Journal of Applied Mechanics*, vol. 18, no. 1, pp. 31–38, Apr. 2021, https://doi.org/10.1115/1.4010217.

[7] T. A. Anderson, "A 3-D elasticity solution for a sandwich composite with functionally graded core subjected to transverse loading by a rigid sphere," *Composite Structures*, vol. 60, no. 3, pp. 265–274, May 2003, https://doi.org/10.1016/S0263-8223(03)00013-8.

[8] S. K. Jalali, M. H. Naei, and A. Poorsolhjouy, "Thermal stability analysis of circular functionally graded sandwich plates of variable thickness using pseudo-spectral method," *Materials & Design*, vol. 31, no. 10, pp. 4755–4763, Dec. 2010, https://doi.org/10.1016/j.matdes.2010.05.009.

[9] S. K. Jalali, M. H. Naei, and A. Poorsolhjouy, "Buckling of circular sandwich plates of variable core thickness and fgm face sheets," *International Journal of Structural Stability and Dynamics*, vol. 11, no. 02, pp. 273–295, Apr. 2011, https://doi.org/10.1142/S0219455411004099.

[10] N. D. Duc, K. Seung-Eock, and D. Q. Chan, "Thermal buckling analysis of FGM sandwich truncated conical shells reinforced by FGM stiffeners resting on elastic foundations using FSDT," *Journal of Thermal Stresses*, vol. 41, no. 3, pp. 331–365, Mar. 2018, https://doi.org/10.1080/01495739.2017.1398623.

[11] M. Yaqoob Yasin and S. Kapuria, "An efficient layerwise finite element for shallow composite and sandwich shells," *Composite Structures*, vol. 98, pp. 202–214, Apr. 2013, https://doi.org/10.1016/j.compstruct.2012.10.048.

[12] N. Grover, B. N. Singh, and D. K. Maiti, "Analytical and finite element modeling of laminated composite and sandwich plates: An assessment of a new shear deformation theory for free vibration response," *International Journal of Mechanical Sciences*, vol. 67, pp. 89–99, Feb. 2013, https://doi.org/10.1016/j.ijmecsci.2012.12.010.

[13] E. Carrera, S. Brischetto, and A. Robaldo, "Variable Kinematic Model for the Analysis of Functionally Graded Material plates," *AIAA Journal*, vol. 46, no. 1, pp. 194–203, Jan. 2008, https://doi.org/10.2514/1.32490.

[14] G. Taj and A. Chakrabarti, "Static and Dynamic Analysis of Functionally Graded Skew Plates," *Journal of Engineering Mechanics*, vol. 139, no. 7, pp. 848–857, Jul. 2013, https://doi.org/10.1061/(ASCE)EM.1943-7889.0000523.

[15] M. N. A. Gulshan Taj, A. Chakrabarti, and A. H. Sheikh, "Analysis of functionally graded plates using higher order shear deformation theory," *Applied Mathematical Modelling*, vol. 37, no. 18, pp. 8484–8494, Oct. 2013, https://doi.org/10.1016/j.apm.2013.03.058.

[16] V. Kahya and M. Turan, "Finite element model for vibration and buckling of functionally graded beams based on the first-order shear deformation theory," *Composites Part B: Engineering*, vol. 109, pp. 108–115, Jan. 2017, https://doi.org/10.1016/j.compositesb.2016.10.039.

[17] M. Bouamama, K. Refassi, A. Elmeiche, and A. Megueni, "Dynamic Behavior of Sandwich FGM Beams," *Mechanics and Mechanical Engineering*, vol. 22, pp. 919–930, Sep. 2020, https://doi.org/10.2478/mme-2018-0072.